

Decaying Dark Matter can explain the e^\pm excesses

Enrico Nardi^{a,b}, Francesco Sannino^c, Alessandro Strumia^d

^a *INFN-Laboratori Nazionali di Frascati, C.P. 13, I-00044 Frascati, Italia*

^b *Instituto de Física, Universidad de Antioquia, A.A.1226 Medellín, Colombia*

^c *Centre for High Energy Physics, University of Southern Denmark, Denmark*

^d *Dipartimento di Fisica dell' Università di Pisa and INFN, Italia*

Abstract

PAMELA and ATIC recently reported excesses in e^\pm cosmic rays. Since the interpretation in terms of DM annihilations was found to be not easily compatible with constraints from photon observations, we consider the DM decay hypothesis and find that it can explain the e^\pm excesses compatibly with all constraints, and can be tested by dedicated HESS observations of the Galactic Ridge. ATIC data indicate a DM mass of about 2 TeV: this mass naturally implies the observed DM abundance relative to ordinary matter if DM is a quasi-stable composite particle with a baryon-like matter asymmetry. Technicolor naturally yields these type of candidates.

1 Introduction

The recent observations of Cosmic Ray e^\pm spectra by PAMELA [1] and ATIC [2] indicate an excess, compatibly with other recent results [3, 4]. Unless it is due to pulsars or some other astrophysical source, this excess could be the first non-gravitational manifestation of Dark Matter. However, the interpretation in terms of DM annihilations into SM particles is possible only for a restricted class of DM models [5, 6, 7, 8] leading to an unobserved excess of gamma or radio photons, unless the DM density profile is significantly less steep than the NFW profile at galactocentric radii below 100 pc [9].

In this paper we show that the interpretation in terms of DM decays [10] circumvents these issues. In section 2 we compute the ‘halo functions’ that encode the astrophysical information relevant for understanding the energy spectra of e^\pm and \bar{p} produced by DM decays. In section 3 we propose a model-independent interpretation of the PAMELA and ATIC observations in terms of DM decays, taking into account constraints from \bar{p} data. In section 4 we show that the models that can explain the PAMELA and ATIC excesses are compatible with photon observations at gamma and radio frequencies, and single out the future observations capable of testing the decaying DM interpretation. We will find that:

- When interpreted in terms of decaying DM, PAMELA e^+ and ATIC $e^+ + e^-$ data can be accounted for by a DM particle with mass around 2 TeV and lifetime $\approx 10^{26}$ s. Decay modes yielding hadrons are constrained by PAMELA \bar{p} data and should not exceed 10%.

In section 5 we explore the possible theoretical realizations of such scenario, finding that:

- If DM particles carry an anomalous global charge B' , the observed DM abundance, $\Omega_{\text{DM}}/\Omega_B \approx 5$, is naturally obtained for $M_{\text{DM}} \approx 2$ TeV.
- The above situation can be realized assuming that DM is a composite state, suggesting a connection with technicolor: if the hypothetical DM is the lightest state carrying technibaryon number B' , a naive rescaling of QCD suggests a $M_{\text{DM}} \approx 2$ TeV mass.
- If B' is violated by dimension-6 higher dimensional operators suppressed by some ‘GUT scale’ $\approx 10^{16}$ GeV, DM is quasi-stable and the desired DM life-time is naturally obtained.

Section 6 summarizes our results.

2 Astrophysics

The computation of the fluxes of SM particles $k = \{e^+, \bar{p}, \dots\}$ from DM decays is analogous to the case of DM annihilations: in brief one needs to replace the ‘annihilations’ source term

$$Q_k(\vec{x}, E) = \frac{1}{2} \left(\frac{\rho(\vec{x})}{M_{\text{DM}}} \right)^2 \langle \sigma v \rangle \frac{dN_k}{dE} \quad (\text{DM annihilations}) \quad (1)$$

with

$$Q_k(\vec{x}, E) = \frac{\rho(\vec{x})}{M_{\text{DM}}} \Gamma \frac{dN_k}{dE} \quad (\text{DM decays}). \quad (2)$$

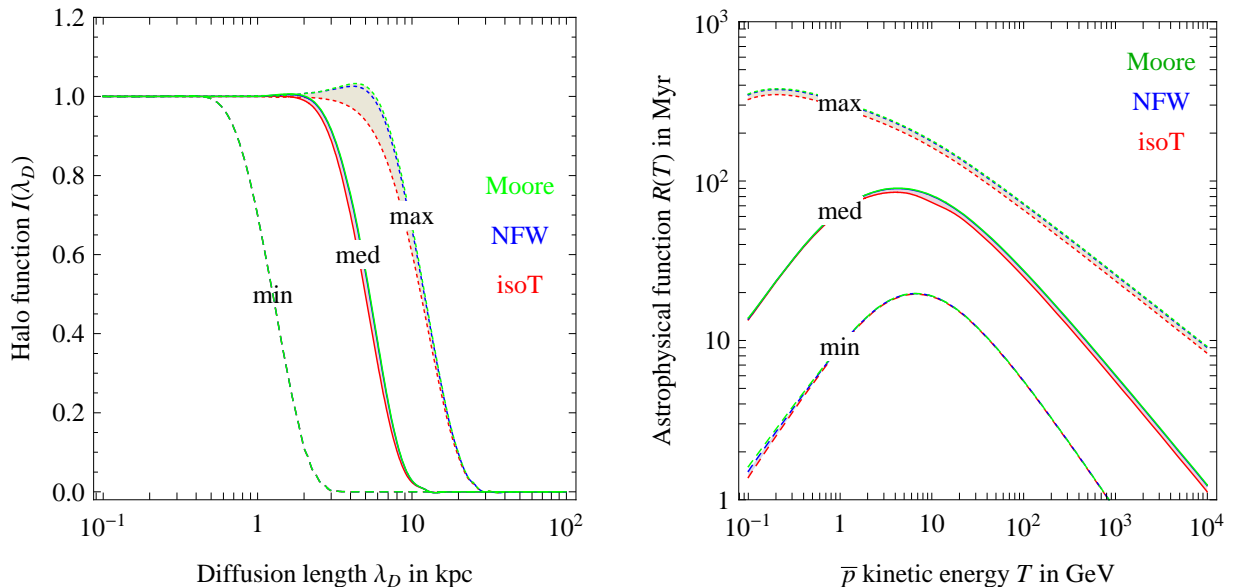


Figure 1: *Left: The uncertain ‘halo function’ $I(\lambda_D)$ of eq. (5) that encodes the astrophysics of DM decays into positrons and their propagation to the Earth. The diffusion length is related to energy losses as in eq. (6). Right: The \bar{p} astrophysical function $R(T)$ of eq. (10), computed under different assumptions. In both cases, the dashed (solid) [dotted] bands assumes the min (med) [max] propagation configuration of eq. (4) and eq. (9) respectively. Each band contains 3 lines, that correspond to the isothermal (red lower lines), NFW (blue middle lines) and Moore (green upper lines) DM density profiles.*

where dN_k/dE is the spectrum of particles k produced by one decay or annihilation, $\rho(\vec{x})$ the DM energy density at \vec{x} and M_{DM} its mass. Furthermore DM sub-halos can enhance the DM annihilation signals by a potentially large ‘boost factor’ $B_k \geq 1$; for DM decays one expects a boost factor negligibly different from unity.

We briefly summarize aspects of e^\pm and p^\pm in our galaxy in order to present the astrophysical functions, plotted in fig. 1, that allow to compute their fluxes at Earth in the generic case.

2.1 Positron propagation

The flux per unit energy of ultra-relativistic positrons is given by $\Phi_{e^+}(t, \vec{x}, E) = f/4\pi$ where the positron number density per unit energy, $f(t, \vec{x}, E) = dN_{e^+}/dE$, obeys the stationary diffusion-loss equation:

$$-K(E) \cdot \nabla^2 f - \frac{\partial}{\partial E} (b(E)f) = Q_e \quad (3)$$

with diffusion coefficient $K(E) = K_0(E/\text{GeV})^\delta$ and energy loss coefficient $b(E) = E^2/(\text{GeV} \cdot \tau_E)$ with $\tau_E = 10^{16}$ s. They respectively describe transport through the turbulent magnetic fields and energy loss due to synchrotron radiation and inverse Compton scattering on galactic photons. Eq. (3) is solved in a diffusive region with the shape of a solid flat cylinder that

sandwiches the galactic plane, with height $2L$ in the z direction and radius $R = 20$ kpc in the r direction. The location of the solar system corresponds to $\vec{x} = (r_\odot, z_\odot) = ((8.5 \pm 0.5) \text{ kpc}, 0)$. The boundary conditions impose that the positron density f vanishes on the surface of the diffusive cylinder, outside of which turbulent magnetic fields can be neglected so that positrons freely propagate and escape. The values of the propagation parameters δ , K_0 and L are deduced from a variety of cosmic ray data and modelizations. We adopt the sets discussed in [11]:

Model	δ	K_0 in kpc ² /Myr	L in kpc
min	0.55	0.00595	1
med	0.70	0.0112	4
max	0.46	0.0765	15

(4)

Analogously to the DM annihilation case [6, 11, 12], the solution for the positron flux at Earth can be written in a useful semi-analytical form

$$\Phi_{e^+}(E, \vec{r}_\odot) = \frac{\Gamma}{4\pi b(E)} \frac{\rho_\odot}{M_{\text{DM}}} \int_E^{M_{\text{DM}}} dE' \frac{dN_{e^+}}{dE'} \cdot I(\lambda_D(E, E')) \quad (5)$$

where $\lambda_D(E, E')$ is the diffusion length from energy E' to energy E :

$$\lambda_D^2 = 4K_0\tau_E \left[\frac{(E'/\text{GeV})^{\delta-1} - (E/\text{GeV})^{\delta-1}}{\delta - 1} \right] \quad (6)$$

the adimensional ‘halo function for DM decays’ $I(\lambda_D)$ fully encodes the galactic astrophysics and is independent on the particle physics model. Its possible shapes are plotted in fig. 1 for the set of DM density profiles (isothermal, Navarro, Frank and White (NFW) [13] and Moore [14]) and e^+ propagation models that we consider. We see that, unlike in the case of DM annihilations, I is negligibly affected by the uncertainty in the DM density profile, and DM decays in the center of the galaxy (at 8.5 kpc from us) are never dominant.

2.2 Antiproton propagation

The propagation of anti-protons through the galaxy is described by a diffusion equation analogous to the one for positrons. Again, the number density of anti-protons per unit energy $f(t, \vec{x}, T) = dN_{\bar{p}}/dT$ vanishes on the surface of the cylinder at $z = \pm L$ and $r = R$. $T = E - m_p$ is the \bar{p} kinetic energy, conveniently used instead of the total energy E . Since $m_p \gg m_e$ we can neglect the energy loss term, and the diffusion equation for f is

$$-K(T) \cdot \nabla^2 f + \frac{\partial}{\partial z} (\text{sign}(z) f V_{\text{conv}}) = Q_p - 2h \delta(z) \Gamma_{\text{ann}} f \quad (7)$$

where:

- The diffusion term can again be written as $K(T) = K_0 \beta (p/\text{GeV})^\delta$, where p and β are the antiproton momentum and velocity. δ and K_0 are given in table (9).
- The V_{conv} term corresponds to a convective wind, assumed to be constant and directed outward from the galactic plane, that tends to push away \bar{p} with energy $T \lesssim 10 m_p$. Its value is given in (9).

- The last term in eq. (7) describes the annihilations of \bar{p} on interstellar protons in the galactic plane (with a thickness of $h = 0.1 \text{ kpc} \ll L$) with rate $\Gamma_{\text{ann}} = (n_{\text{H}} + 4^{2/3} n_{\text{He}}) \sigma_{p\bar{p}}^{\text{ann}} v_{\bar{p}}$, where $n_{\text{H}} \approx 1/\text{cm}^3$ is the hydrogen density, $n_{\text{He}} \approx 0.07 n_{\text{H}}$ is the Helium density (the factor $4^{2/3}$ accounting for the different geometrical cross section in an effective way) and $\sigma_{p\bar{p}}^{\text{ann}}$ is given by [12]

$$\sigma_{p\bar{p}}^{\text{ann}} = \begin{cases} 661 (1 + 0.0115 T^{-0.774} - 0.984 T^{0.0151}) \text{ mbarn}, & \text{for } T < 15.5 \text{ GeV} \\ 36 T^{-0.5} \text{ mbarn}, & \text{for } T \geq 15.5 \text{ GeV} \end{cases} \quad (8)$$

- We neglect ‘‘tertiary \bar{p} ’’, i.e. non-annihilating \bar{p} interactions on the matter in the galactic disk.

The set of propagation parameters that we adopt in the case for anti-protons has been deduced in [15]:

Model	δ	K_0 in kpc^2/Myr	L in kpc	V_{conv} in km/s
min	0.85	0.0016	1	13.5
med	0.70	0.0112	4	12
max	0.46	0.0765	15	5

(9)

The solution for the antiproton flux at the position of the Earth $\Phi_{\bar{p}}(T, \vec{r}_{\odot}) = v_{\bar{p}}/(4\pi) f$ can be written as

$$\Phi_{\bar{p}}(T, \vec{r}_{\odot}) = \Gamma \frac{v_{\bar{p}}}{4\pi} \frac{\rho_{\odot}}{M_{\text{DM}}} R(T) \frac{dN_{\bar{p}}^k}{dT}, \quad (10)$$

where $\rho_{\odot} \equiv \rho(\vec{r}_{\odot})$. The ‘halo function for DM decays’ $R(T)$ encodes all the astrophysics and is plotted in fig. 1 for the halo and propagation models that we consider. It depends negligibly on the DM density profile, unlike for the analogous function relevant for DM annihilations, plotted in fig. 4 of [6].

3 The PAMELA and ATIC data as DM decays

With the goal of performing a model-independent analysis, we delineate the generic features implied by known physics. We recall that non-relativistic DM annihilations are equivalent to the decay of the s -wave DM two-body state with mass $2M_{\text{DM}}$, that can only have spin 0, 1 or 2, if DM is a weakly-interacting particle [5].

The decay of a DM is less constrained: since DM could be coupled only gravitationally to SM particles, its spin can be anything: 0, 1/2, 1, 3/2, 2, etc. Furthermore, since DM decay must be slow, decays into two SM particles do not need to dominate over multi-body decays; decay rates suppressed by helicity factors such as $(m_e/M_{\text{DM}})^2$ are still phenomenologically interesting; DM decays might involve new particles (e.g. gravitino decays into gluinos and quarks).

At the light of the results of [5] that single out decays into hard leptons as phenomenologically promising we will study the following DM decay modes. For boson DM:

$$\text{DM} \rightarrow e^+e^-, \mu^+\mu^-, \tau^+\tau^-, W^+W^-, t\bar{t}, hh \quad (11)$$

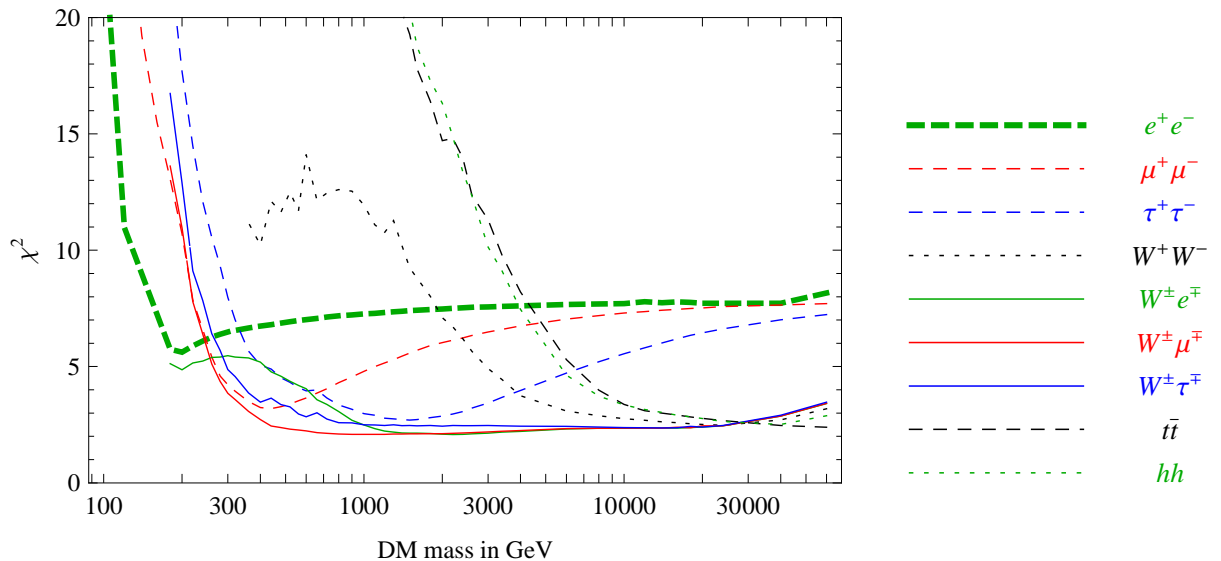


Figure 2: A fit of the DM decays indicated in the legend to the PAMELA positron data.

where the $t\bar{t}$ and hh modes are included as examples of hadronic modes. For fermion DM we consider:

$$\text{DM} \rightarrow W^\pm e^\mp, W^\pm \mu^\mp, W^\pm \tau^\mp. \quad (12)$$

3 body decays, such as $\text{DM} \rightarrow \ell^+ \ell^- \nu$ are also possible, but cannot be computed in a model-independent way.

We fit the PAMELA and ATIC data taking into account as described in [5] the uncertainties on the astrophysical backgrounds, on the e^\pm and \bar{p} propagation, on the DM density profile, on the experimental data.

3.1 PAMELA e^+ data

We start including only the PAMELA data about the positron fraction [1], that exhibit an excess above 10 GeV. Fig. 2 shows the quality of the best-fit as function of the DM mass for the different decay modes we consider, and fig. 3 shows the corresponding best-fit values of the DM life-time, that is $\tau \sim 10^{26}$ sec. The left column of fig. 5 show three possible fits.

3.2 PAMELA e^+ and $e^+ + e^-$ data

Next, we explore the combined fit of PAMELA e^+ and the $e^+ + e^-$ data, as measured by balloon experiments [2] and at higher energies by HESS [4]. We plot and fit the HESS data combining in quadrature a systematic $\pm 20\%$ systematic error with a $\pm 15\%$ energy-scale uncertainty with the statistical uncertainty on each data point [4]. Fig. 4 shows our results: the peak possibly present in the $e^+ + e^-$ energy spectrum, as measured by ATIC-2 and PPB-BETS, strongly restricts the

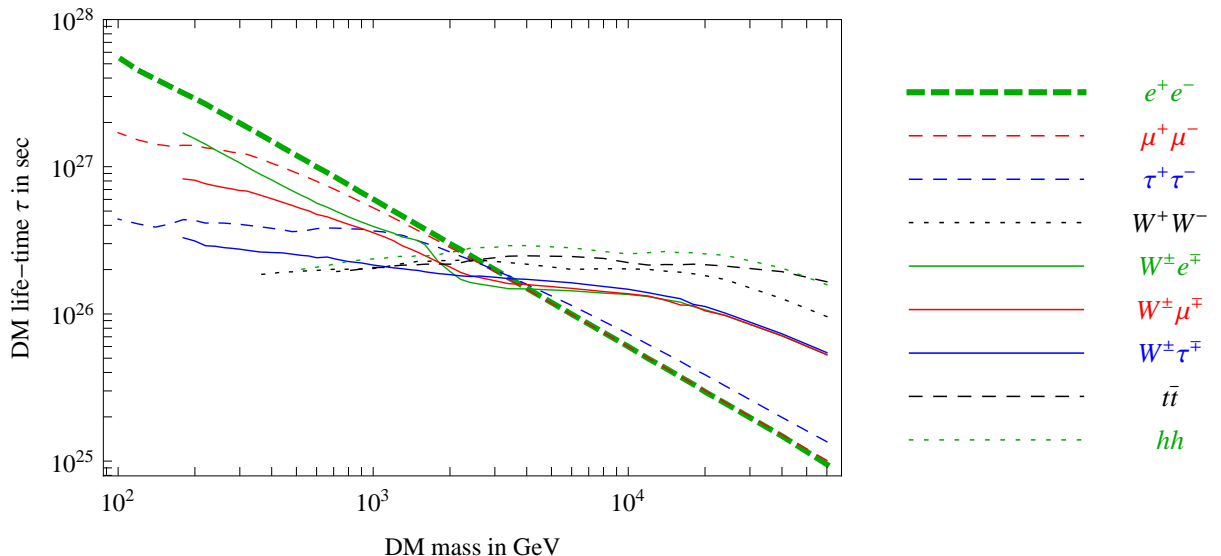


Figure 3: *Best-fit values of the DM life-time suggested by the PAMELA excess, for the DM decay modes indicated on the legend.*

DM mass and the DM decay modes. Like in the DM annihilation case, the $\mu^+\mu^-$ and $\tau^+\tau^-$ modes provide good fits, now for a value of the DM mass twice as large: $M \approx 3$ TeV. Unlike in the DM annihilation case, the e^+e^- mode does not provide a good fit, due to the following detailed argument, that can be weakened invoking additional astrophysical uncertainties. The problem is that the e^\pm line remains too sharp. Indeed DM decays (unlike DM annihilations) are not strongly enhanced close to the galactic center, so that such e^+ produced far from us and that therefore reach us at the price of significant energy losses are now a minor component. Furthermore, the new $W^\pm\ell^\mp$ decay modes possible for fermion DM also provide good fits for e^+ and $e^+ + e^-$ data for any ℓ . A similar result holds for the various 3-body decays $\text{DM} \rightarrow \ell^+\ell^-\nu$, that we cannot compute in a model-independent way.

3.3 PAMELA e^+ and \bar{p} data

Fig. 6 shows the result of the fit of PAMELA e^+ and \bar{p} PAMELA observations. The \bar{p} data, that do not show an excess with respect to the expected astrophysical background, provide significant constraints, disfavoring decay modes that lead to hadrons. The situation with the $\text{DM} \rightarrow W^+W^-, t\bar{t}, hh$ modes is similar to the DM annihilation case [5]: such modes are disfavored unless $M \gtrsim 10$ TeV. We see that the same conclusion applies to the new semi-leptonic decay modes $W^\pm\ell^\mp$: choosing $M \sim 2$ TeV in order to fit the $e^+ + e^-$ peak in ATIC-2 data is disfavored by PAMELA \bar{p} data. This is illustrated in the upper row of fig. 5, where we summed over all leptons $\ell = \{e, \mu, \tau\}$ as suggested by gauge invariance. We recall that we assumed equal propagation models for e^+ and \bar{p} , as controlled by the thickness L of the cylinder where turbulent

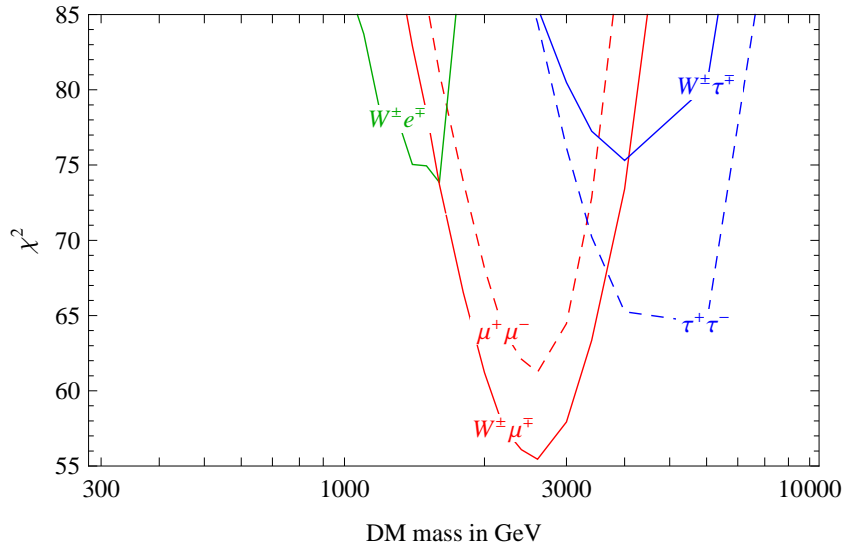


Figure 4: *Combined fit of positron data from PAMELA and of $e^+ + e^-$ data from ATIC, BBP-BETS, EC, HESS.*

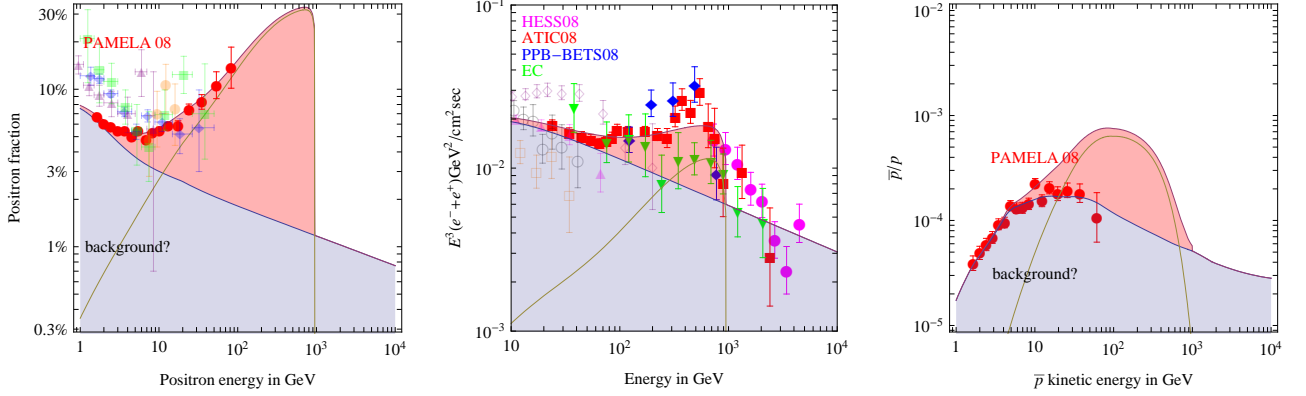
magnetic fields lead to diffusion of charged particles. Our conclusions can be weakened assuming different propagation models for \bar{p} and e^+ . Unlike in the DM annihilation case it is not possible to weaken these conclusions by assuming a boost factor $B_p \ll B_e$.

Summarizing, a good fit to all e^+ , $e^+ + e^-$ and \bar{p} CR data presently available in terms of decaying DM requires decays into $\mu^+\mu^-$ or $\tau^+\tau^-$, which are possible if DM is a boson. A fermion DM can decay into $\ell^+\ell^-\nu$, which can also provide a good global fit, although we cannot compute the resulting e^\pm energy spectra in a model-independent way. If decaying DM is only a fraction f of all DM, our results still hold up to the rescaling $\tau \rightarrow \tau/f$.

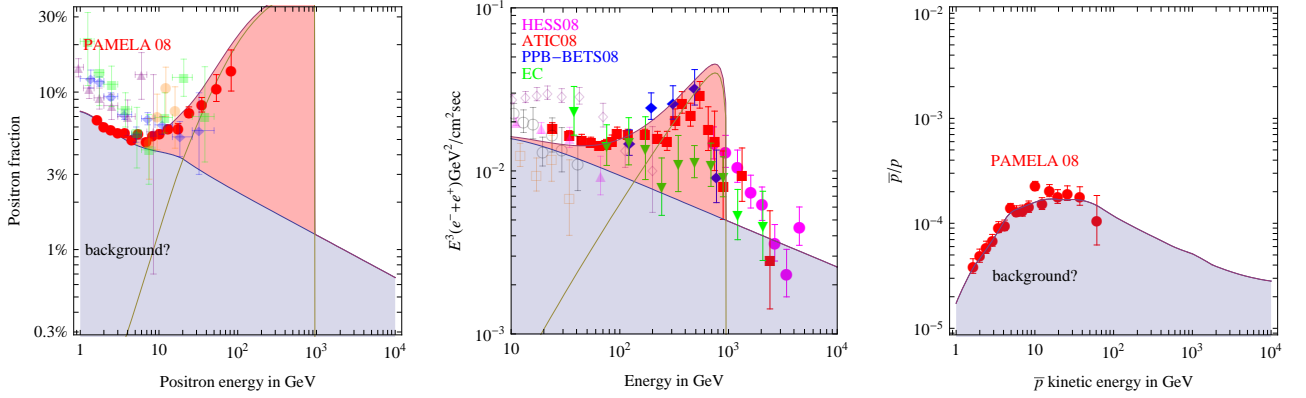
4 Photons: bounds and signals

DM decays unavoidably lead to photons: at γ frequencies due to brehmstrahlung of charged particles, and at radio frequencies due to synchrotron radiation emitted by e^\pm in the galactic magnetic fields. Here we compare the flux of photons produced by DM decays with the existing bounds and we comment on future perspectives. There are three main robust constraints and we find that, unlike in the case of DM annihilations [9], they are satisfied even in the case of a NFW DM density profile.

DM with $M = 2$ TeV that decays into $W^\pm \ell^\mp$



DM with $M = 2$ TeV that decays into e^+e^-



DM with $M = 4$ TeV that decays into $\tau^+\tau^-$

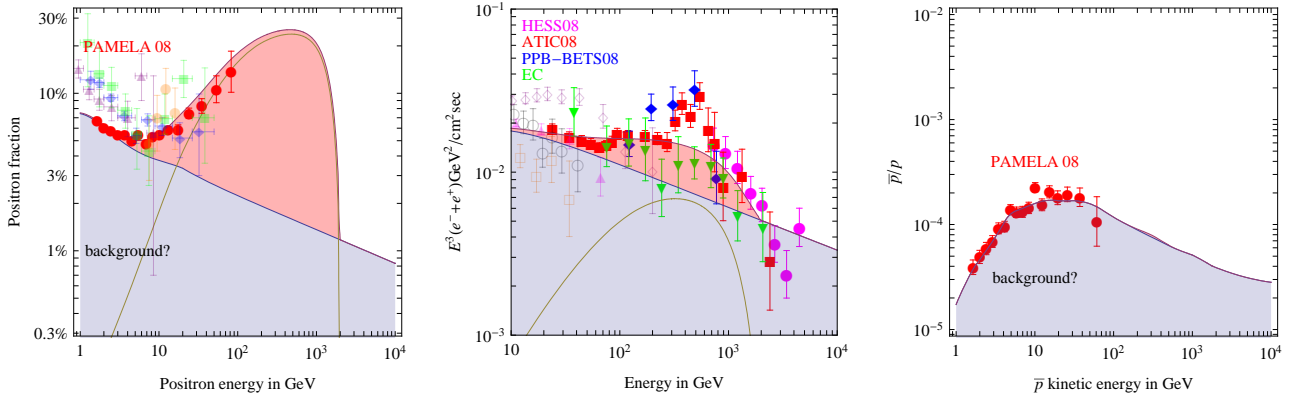


Figure 5: Examples of fits of e^+ (left), $e^+ + e^-$ (center), \bar{p} (right) CR data, for DM decay modes into $W^\pm \ell^\mp$ (that leads to an unseen \bar{p} excess), e^+e^- (that leads to a too sharp peak), $\tau^+\tau^-$ (that leads to peak less sharp than suggested by ATIC data). A combination of the last two possibilities, and the intermediate $\text{DM} \rightarrow \mu^+\mu^-$ decay gives the optimal fit.

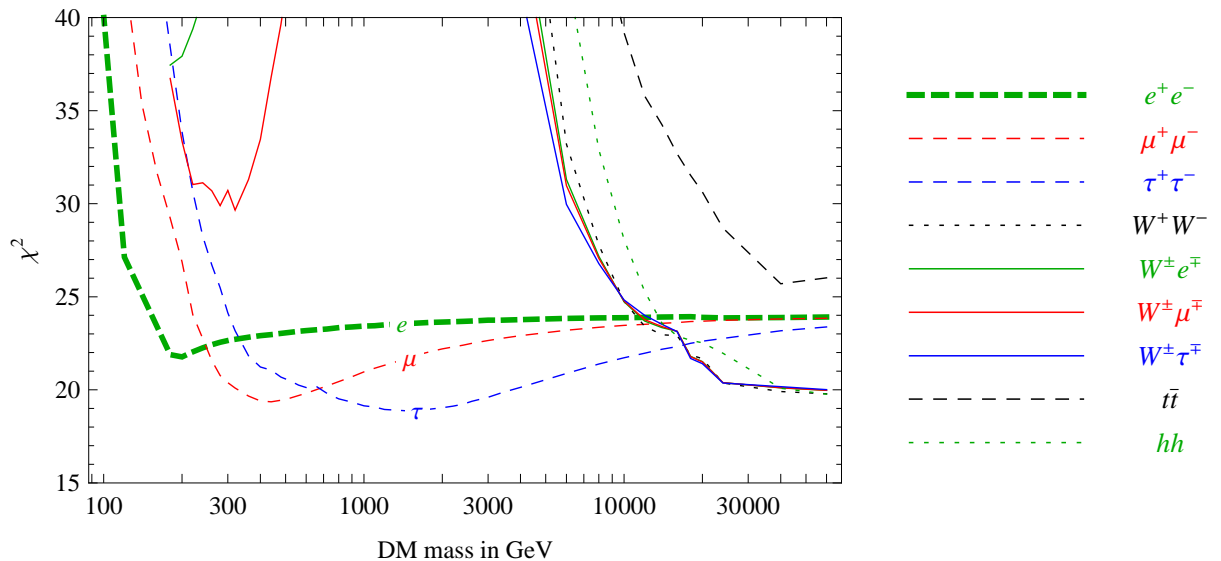


Figure 6: Combined fit of different DM decay channels to the PAMELA positron and PAMELA anti-proton data, assuming equal propagation models for e^\pm and \bar{p} .

4.1 HESS observation of the Galactic Center

The differential flux of photons received from a given angular direction $d\Omega$ is

$$\frac{d\Phi_\gamma}{d\Omega dE} = \Gamma \frac{r_\odot \rho_\odot}{4\pi M} \frac{dN_\gamma}{dE} \frac{dJ}{d\Omega}, \quad \frac{dJ}{d\Omega} = \int_{\text{line-of-sight}} \frac{ds}{r_\odot} \frac{\rho}{\rho_\odot} \quad (13)$$

where dN_γ/dE is the photon spectrum produced in one DM decay: we here include only the model-independent contribution due to brehmstralung of charged particles. We conservatively impose that such contribution does not exceed at 3σ the observed flux in any data-point. The adimensional quantity J describes the uncertain astrophysics. Observing an angular region $\Delta\Omega = 10^{-5}$ centered on the GC, we find

$$\text{GC } J \text{ for DM decays} = \{5.75, 28.9, 45.3\} \quad \text{for the \{isoT, NFW, Moore\} profiles} \quad (14)$$

for the quantity J defined by $J \cdot \Delta\Omega = \int d\Omega \cdot dJ/d\Omega$. In the case of DM annihilations, one instead has $J \cdot \Delta\Omega = \int d\Omega \int (\rho/\rho_\odot)^2 ds/r_\odot$ and, the analogous factor J acquires much larger values, such as $J = 14700$ for the NFW profile, implying that the PAMELA anomaly is not compatible with bounds from γ observations, unless DM is distributed with an isothermal-like profile and/or the e^\pm signal is enhanced by a large boost factor $B_e \gtrsim 10^2 \gg B_\gamma$ [9].

On the contrary this problematic issue is not present for the DM decay interpretation of the PAMELA excess, as shown by the blue continuous lines in fig.s 7.

4.2 HESS observation of the Galactic Ridge

It is unclear which observation region gives the maximal sensitivity to γ rays from DM decays. Observing the Galactic Center (GC) maximizes the signal rate, especially for cusped profiles such as NFW, where the DM density ρ grows as $1/r$ as $r \rightarrow 0$, and especially for DM annihilations, where the signal rate is proportional to ρ^2 . However, the GC also has the highest background rate, as HESS observations suggest that it is polluted by astrophysical sources of γ rays.

For DM decays, the signal is proportional to ρ rather than to ρ^2 , so the optimal strategy might be instead observing a larger region. HESS observed the Galactic Ridge (GR), defined as the region corresponding to longitude $|\ell| < 0.8^\circ$ and latitude $|b| < 0.3^\circ$, with a cone of angle 0.1° centered on the GC subtracted.

This HESS observation leads to the dominant constraint on DM decays. Indeed HESS finds comparable total γ fluxes from the GC and the GR regions, $d\Phi_{\text{GR}}/dE_\gamma \sim 3d\Phi_{\text{CG}}/dE_\gamma$, and we find comparable values of J :

$$\text{GR } J \text{ for DM decays} = \{5.55, 20.5, 26.8\} \quad \text{for the \{isoT, NFW, Moore\} profiles.} \quad (15)$$

Therefore, since $\Delta\Omega_{\text{GR}} \sim 30\Delta\Omega_{\text{GC}}$, observations of the GR set a bound on the DM life-time τ which is about 10 times stronger than the GC bound. The blue dot-dashed lines in fig. 7 show our precise result.

The GR HESS bound is close to the value of the DM life-time τ suggested by PAMELA/ATIC. Such bound can presumably be improved by observing some region away from the Galactic Plane, to be chosen trying to avoid the astrophysical background. Unfortunately, astrophysicists are interested in astrophysical ‘backgrounds’, so that the GR region observed by HESS, that contains the galactic plane, is clearly not the optimal choice.

4.3 HESS observation of Sagittarius Dwarf

Dwarf spheroidals are among the most DM-dominated structures, so that they allow to search for γ ray signals of DM annihilations with minimal astrophysical backgrounds. HESS observed Sagittarius Dwarf at distance $d = 24$ kpc from us for a time $T_{\text{obs}} = 11$ h in a region with angular size $\Delta\Omega = 2 \cdot 10^{-5}$, finding no γ excess and setting the bound $N_\gamma \lesssim 85$ at about 3σ . The γ flux from DM decays is

$$\frac{d\Phi_\gamma}{dE} = \frac{\Gamma}{M} \frac{dN_\gamma}{dE} \frac{1}{4\pi d^2} \int_{\text{cone}} dV \rho, \quad N_\gamma = T_{\text{obs}} \int dE A_{\text{eff}}(E) \frac{d\Phi_\gamma}{dE} \quad (16)$$

where $A_{\text{eff}}(E) \sim 10^5 \text{ m}^2$ is the effective area of HESS [16]. The integral is the total DM mass \mathcal{M} contained in the volume observed by HESS, and is equal to $\mathcal{M} \approx 5 \cdot 10^6 M_\odot$ assuming a NFW or cored density profile [17] for Sagittarius Dwarf. Therefore, the bound on the DM life-time is:

$$\tau > \frac{T_{\text{obs}}}{N_\gamma^{\text{max}}} \frac{\mathcal{M}}{M} \frac{1}{4\pi d^2} \int dE A_{\text{eff}}(E) \frac{dN_\gamma}{dE}. \quad (17)$$

The resulting bound are plotted in fig.s 7 as blue dotted lines.

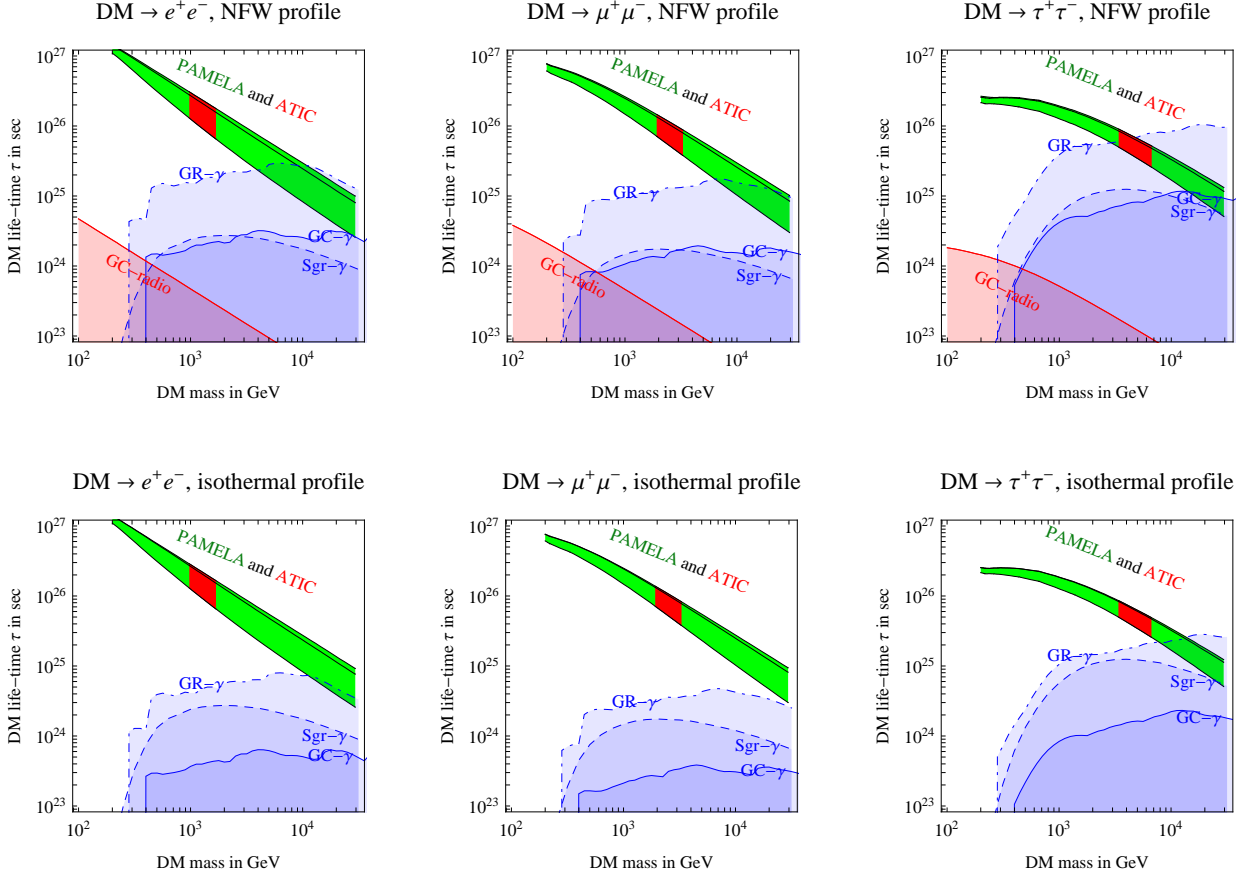


Figure 7: Assuming Dark Matter decays into e^+e^- (left column), $\mu^+\mu^-$ (middle column), $\tau^+\tau^-$ (right column) we compare the region favored by PAMELA (green band) and ATIC (red region), as computed for min/max/med e^\pm galactic propagation, with the bounds from HESS gamma observations of the Galactic Center (blue continuous curves), of the Galactic Ridge (dot-dashed curves) of Sagittarius Dwarf (blue dashed curves), and with radiowave observations of the Galactic Center. We assumed NFW (upper row) and isothermal (lower row) DM density profiles.

4.4 Synchrotron radiation from the Galactic Center

The e^\pm produced by DM decays within the galactic magnetic field radiate synchrotron radiation. As the galactic magnetic fields are poorly known, in order to discuss which bounds are robust we recall the basic physics. One expects $B \sim \mu\text{G}$ that grows to higher values close to the galactic center. Such magnetic fields are intense enough that e^\pm radiate an order unity fraction of their energy into synchrotron radiation, as other energy losses and diffusion are not the main phenomena. Therefore the total energy into synchrotron radiation can be robustly computed, and the value of the magnetic field only determines how it is distributed in the frequency spectrum. We recall that the synchrotron power W_γ radiated orthogonally to the magnetic field B by an e^\pm with momentum p is:

$$\frac{dW_{\text{syn}}}{d\nu} \approx \frac{2e^3 B}{9m_e} \delta\left(\frac{\nu}{\nu_{\text{syn}}} - \frac{1}{3}\right) \quad \text{where} \quad \nu_{\text{syn}} = \frac{3eBp^2}{4\pi m_e^3} = 4.2 \text{ MHz} \frac{B}{\text{G}} \left(\frac{p}{m_e}\right)^2. \quad (18)$$

Thereby a larger magnetic field and heavier DM mean that synchrotron radiation extends up to higher energy. In order to put a robust bound, we consider the observation [18] of the GC in a region with angular size $4''$ at the lowest radio-wave frequency $\nu = 0.408 \text{ GHz}$, that implies the bound $S = (\nu dW_{\text{syn}}/d\nu)/(4\pi r_\odot^2) < 2 \cdot 10^{-16} \text{ erg/cm}^2\text{sec}$. This is the relevant bound, as the observed GC microwave spectrum is harder than what DM decays can produce. The region is large enough that we can neglect e^\pm diffusion and advection (e^\pm falling in the central black hole). In this approximation the electron number density is given by $n_e(r, p) \simeq \dot{E}_{\text{syn}}^{-1} \int_E^\infty dE' Q_e(r, E')$ with $\dot{E}_{\text{syn}} = e^4 B^2 p^2 / 9\pi m_e^4$ is the synchrotron energy loss of a e^\pm in a turbulent magnetic field. So

$$\nu \frac{dW_{\text{syn}}}{d\nu} = \frac{\Gamma}{M} \int_{\text{cone}} dV \rho p N_e(p) \quad (19)$$

where the integral extends over the observed volume and p is obtained from eq.s (18) as $p = \sqrt{4\pi m_e^3 \nu / B} = 0.43 \text{ GeV} (\nu/\text{GHz})^{1/2} (B/\text{mG})^{-1/2}$. Here, $N_e(p)$ is the number of electrons with energy above p produced in one DM decay, and can be often approximated as the total number of electrons produced in one DM decay. As anticipated at the beginning of this section, a lower B leads to a higher synchrotron flux at the low frequency we consider.

Observations are made at scales large enough that the dipolar structure of the GC can be neglected: we model the GC as in [9] in ‘spherical-cow’ approximation, obtaining the bounds plotted as red lines in fig.s 7. The radio-wave constraints turn out to be subdominant with respect to the γ -ray constraints previously computed.

5 Theory

In the DM annihilation case, model building is needed to invent models of DM that annihilate dominantly into leptons with cross section larger than the one suggested by cosmology. Key ingredients of such models are the Sommerfeld enhancement and possibly new vectors that decay into leptons [5, 6, 7].

DM decay allows to circumvent such model-building issues. It is very easy to invent models of DM that decays dominantly to leptons, and small couplings to leptons might be somehow connected to the small observed neutrino masses and baryon/lepton cosmological asymmetries.

One example is analogous to type-II see-saw [19]: DM might be a scalar $SU(2)_L$ triplet T with Lagrangian couplings $M^2 T T^* + \lambda_L T L L + M \lambda_T T H H$, so that it dominantly decays into leptons if $\lambda_L \gg \lambda_T$. Alternatively, along the lines of type-I or type-III see-saw [19], one can introduce fermion singlets or triplets N and an inert Higgs H' with couplings (for simplicity we consider the supersymmetric case and write the superpotential) $M N^2/2 + \lambda N L H' + \epsilon N^3$. The neutral component of H' could be DM and decay into $L \bar{L} L$ with a slow rate suppressed by $(\epsilon/M)^2$. Within supersymmetry, one can build models of gravitino DM that decays into leptons, by assuming an appropriate sparticle spectrum and that $L L E$ operators dominate R -parity violation. DM might be some Froggatt-Nielsen-like field, and its slow decays into leptons might be related to the quasi-conserved $U(1)_\ell$ flavor lepton numbers present in the lepton sector.

We now focus on a more interesting idea.

5.1 Non-annihilating DM and the $\Omega_{\text{DM}}/\Omega_B$ ratio

A rather attractive scenario for decaying DM arises when one tries to relate the DM and the baryon energy densities in order to explain the ratio $\Omega_{\text{DM}}/\Omega_B \sim 5$ [20].

We know that the amount of baryons in the Universe $\Omega_B \sim 0.04$ is determined solely by the cosmic baryon asymmetry $n_B/n_\gamma \sim 6 \times 10^{-10}$. This is because the baryon-antibaryon annihilation cross section is so large, that virtually all antibaryons annihilate away, and only the contribution proportional to the asymmetry remains. This asymmetry can be dynamically generated after inflation. In contrast, we do not know if the DM density is determined by thermal freeze-out, by an asymmetry, or by something else. Thermal freeze-out needs a $\sigma v \approx 3 \cdot 10^{-26} \text{ cm}^3/\text{sec}$ of electroweak size, suggesting a DM mass in the TeV range. If Ω_{DM} is determined by thermal freeze-out, its proximity to Ω_B is just a fortuitous coincidence and is left unexplained.

If instead $\Omega_{\text{DM}} \sim \Omega_B$ is not accidental, then the theoretical challenge is to define a consistent scenario in which the two energy densities are related. Since Ω_B is a result of an asymmetry, then relating the amount of DM to the amount of baryon matter can very well imply that Ω_{DM} is related to the same asymmetry that determines Ω_B . Such a condition is straightforwardly realized if the asymmetry for the DM particles is fed in by the non-perturbative electroweak sphaleron transitions, that at temperatures much larger than the temperature T_* of the electroweak phase transition (EWPT) equilibrates the baryon, lepton and DM asymmetries. Implementing this condition implies the following requirements:

1. DM must be (or must be a composite state of) a fermion, chiral (and thereby non-singlet) under the weak $SU(2)_L$, and carrying an anomalous (quasi)-conserved quantum number B' .
2. DM (or its constituents) must have an annihilation cross section much larger than electroweak $\sigma_{\text{ann}} \gg 3 \cdot 10^{-26} \text{ cm}^3/\text{sec}$, to ensure that Ω_{DM} is determined dominantly by the B' asymmetry.

The first condition ensures that a global quantum number corresponding to a linear combination of B , L and B' has a weak anomaly, and thus DM carrying B' charge is produced in anomalous processes together with left-handed quarks and leptons [21, 22]. At temperatures

$T \gg T_*$ electroweak anomalous processes are in thermal equilibrium, and equilibrate the various asymmetries $Y_{\Delta B} = c_L Y_{\Delta L} = c_{B'} Y_{\Delta B'} \sim \mathcal{O}(10^{-10})$. Here the Y_{Δ} 's represent the difference in particle number densities $n - \bar{n}$ normalized to the entropy density s , e.g. $Y_{\Delta B} = (n_B - \bar{n}_B)/s$. These are convenient quantities since they are conserved during the Universe thermal evolution.

At $T \gg M_{\text{DM}}$ all particle masses can be neglected, and c_L and $c_{B'}$ are order one coefficients, determined via chemical equilibrium conditions enforced by elementary reactions faster than the Universe expansion rate [23]. These coefficients can be computed in terms of the particle content, finding e.g. $c_L = -28/51$ in the SM and $c_L = -8/15$ in the MSSM.

At $T \ll M_{\text{DM}}$, the B' asymmetry gets suppressed by a Boltzmann exponential factor $e^{-M_{\text{DM}}/T}$. A key feature of sphaleron transitions is that their rate gets suddenly suppressed at some temperature T_* slightly below the critical temperature at which $\text{SU}(2)_L$ starts to be spontaneously broken. Thereby, if $M_{\text{DM}} < T_*$ the B' asymmetry gets frozen at a value of $\mathcal{O}(Y_{\Delta B})$, while if instead $M_{\text{DM}} > T_*$ it gets exponentially suppressed as $Y_{\Delta B'}/Y_{\Delta B} \sim e^{-M_{\text{DM}}/T}$.

More in detail, the sphaleron processes relate the asymmetries of the various fermionic species with chiral electroweak interactions as follows. If B' , B and L are the only quantum numbers involved then the relation is:

$$\frac{Y_{\Delta B'}}{Y_{\Delta B}} = c \cdot \mathcal{S} \left(\frac{M_{\text{DM}}}{T_*} \right), \quad c = \bar{c}_{B'} + \bar{c}_L \frac{Y_{\Delta L}}{Y_{\Delta B}}, \quad (20)$$

where the order-one $\bar{c}_{L,B'}$ coefficients are related to the $c_{L,B'}$ above in a simple way. The explicit numerical values of these coefficients depend also on the order of the finite temperature electroweak phase transition via the imposition or not of the weak isospin charge neutrality. In [24, 25] the dependence on the order of the electroweak phase transition was studied in two explicit models, and it was found that in all cases the coefficients remain of order one. The statistical function \mathcal{S} is:

$$\mathcal{S}(z) = \begin{cases} \frac{6}{4\pi^2} \int_0^\infty dx x^2 \cosh^{-2} \left(\frac{1}{2} \sqrt{x^2 + z^2} \right) & \text{for fermions,} \\ \frac{6}{4\pi^2} \int_0^\infty dx x^2 \sinh^{-2} \left(\frac{1}{2} \sqrt{x^2 + z^2} \right) & \text{for bosons.} \end{cases} \quad (21)$$

with $S(0) = 1(2)$ for bosons (fermions) and $S(z) \simeq 12 (z/2\pi)^{3/2} e^{-z}$ at $z \gg 1$. We assumed the Standard Model fields to be relativistic and checked that this is a good approximation even for the top quark [25, 24]. The statistic function leads to the two limiting results:

$$\frac{Y_{\Delta B'}}{Y_{\Delta B}} = c \times \begin{cases} \mathcal{S}(0) & \text{for } M_{\text{DM}} \ll T_* \\ 12 (M_{\text{DM}}/2\pi T_*)^{3/2} e^{-M_{\text{DM}}/T_*} & \text{for } M_{\text{DM}} \gg T_* \end{cases}. \quad (22)$$

Under the assumption that all antiparticles carrying B and B' charges are annihilated away we have $Y_{\Delta B'}/Y_{\Delta B} = n_{B'}/n_B$. The observed DM density

$$\frac{\Omega_{\text{DM}}}{\Omega_B} = \frac{M_{\text{DM}} n_{B'}}{m_p n_B} \approx 5 \quad (23)$$

(where $m_p \approx 1 \text{ GeV}$) can be reproduced for two possible values of the DM mass:

- i) $M_{\text{DM}} \sim 5 \text{ GeV}$ if $M_{\text{DM}} \ll T_*$, times model dependent order one coefficients.

- ii) $M_{\text{DM}} \approx 8T_* \approx 2 \text{ TeV}$ if $M_{\text{DM}} \gg T_*$, with a mild dependence on the model-dependent order unity coefficients.

The first solution is well known [21] and not interesting for our purposes. The second solution matches the DM mass suggested by ATIC, in view of $T_* \sim v$ [22], where $v \simeq 250 \text{ GeV}$ is the value of the electroweak breaking order parameter¹.

5.2 DM mass from strongly interacting dynamics

The ideal DM candidate suggested by the PAMELA and ATIC anomalies, and compatible with direct DM searches, is a $\sim 2 \text{ TeV}$ particle that decays dominantly into leptons, and that has a negligible coupling to the Z .

If DM is an elementary particle, this scenario needs DM to be a chiral fermion with $SU(2)_L$ interactions, which is very problematic. Bounds from direct detection are violated. Furthermore, a Yukawa coupling λ of DM to the Higgs gives the desired DM mass $M_{\text{DM}} \sim \lambda v \sim 2 \text{ TeV}$ if $\lambda \sim 4\pi$ is non-perturbative, hinting to a dynamically generated mass associated to some new strongly interacting dynamics [27, 22, 24, 25]. This assumption also solves the problem with direct detection bounds, which are satisfied if DM is a composite $SU(2)_L$ -singlet state, made of elementary fermions charged under $SU(2)_L$.

This can be realized by introducing a strongly-interacting ad-hoc ‘hidden’ gauge group. A more interesting identification, namely *technicolor*, is suggested by the the proximity of the DM mass indicated by ATIC, $M_{\text{DM}} \sim 2 \text{ TeV}$, with the $4\pi v$ scale at which strong dynamics might naturally generate the breaking of the electroweak symmetry. In such a scenario, DM would be the lightest (quasi)-stable composite state carrying a B' charge of a theory of dynamical electroweak breaking featuring a spectrum of technibaryons (B') and technipions (Π).

Let us elaborate more quantitatively on this numerical connection. The DM mass can be approximated as $m_{B'} = M_{\text{DM}} \approx n_Q \Lambda_{\text{TC}}$ where n_Q is the number of techniquarks Q bounded into B' and Λ_{TC} is the constituent mass, so that $M_{\text{DM}}/m_p \approx n_Q \Lambda_{\text{TC}}/3\Lambda_{\text{QCD}}$. Denoting by f_π (F_Π) the (techni)pion decay constant, we have $F_\Pi/f_\pi = \sqrt{D/3} \Lambda_{\text{TC}}/\Lambda_{\text{QCD}}$ where D_Q is the dimension of the constituent fermions representation ($D = 3$ in QCD)². Finally, the electroweak breaking order parameter is obtained as $v^2 = N_D F_\Pi^2$, from the sum of the contribution of the N_D electroweak techni-doublets. Putting all together yields the estimate:

$$M_{\text{DM}} \approx \frac{n_Q}{\sqrt{3D_Q N_D}} \frac{v}{f_\pi} m_p = 2.2 \text{ TeV} \quad (24)$$

where the numerical value corresponds to the smallest number of constituents and of techniquarks $n_Q = D_Q = 2$ and $N_D = 1$. We conclude that naive rescaling of QCD yields a value of M_{DM} right in the ballpark suggested by ATIC.³

¹More precisely, for a Higgs mass $m_h = 120(300) \text{ GeV}$, Ref. [26] estimates $T_* \approx 130(200) \text{ GeV}$, where the larger T_* values arise because of the larger values Higgs self coupling. For the large masses that are typical of composite Higgs models, the self coupling is in principle calculable and generally large [25], so that taking $T_* \sim v$ is not unreasonable.

²The large- N counting relevant for a generic extension of technicolor type can be found in Appendix F of [28] together with a general introduction to recent models of dynamical electroweak symmetry breaking.

³Besides to the possibility indicated above, a dynamical origin of the breaking of the electroweak symmetry can lead to several other interesting DM candidates (see [28] for a list of relevant references).

5.3 Phenomenological constraints on techni-DM

It is worth mentioning that models of dynamical breaking of the electroweak symmetry do support the possibility of generating the experimentally observed baryon (and possibly also the technibaryon/DM) asymmetry of the Universe directly at the electroweak phase transition [29]. Electroweak baryogenesis [30] is, however, impossible in the Standard Model [31] (see [32] for a review on this topic).

Bounds from direct detection experiments such as CDMS and XENON suggest that a single component DM candidate can have, at most, a tiny coupling with the photon [33], the Z [34, 35] and the gluons. We therefore assume that our technibaryon B' is a singlet of $SU(2)_L$ with zero hypercharge (and thus also electrically neutral). Being composed of fermions with electroweak interactions, analogously to the neutron, the DM particles will have electro(weak) magnetic dipoles and other similar form factors, that can be parameterized at low energy by non-renormalizable effective operators suppressed by powers of the technicolor scale Λ_{TC} . For example, if the B' particle is a composite scalar, the relevant operators are suppressed at least by two powers of Λ_{TC} [36], and it has been checked in [24] that in this case the expected interaction rate remains below the present bounds [37]. An interesting collection of other techno-cosmology estimates can be found in [27].

5.4 DM lifetime and decay modes

According to [38] the sphaleron contribution to the techni-baryon decay rate is negligible because exponentially suppressed, unless the techni-baryon is heavier than several TeV.

Grand unified theories (GUTs) suggest that the baryon number B is violated by dimension-6 operators suppressed by the GUT scale $M_{\text{GUT}} \sim 2 \cdot 10^{16}$ GeV, yielding a proton life-time [39]

$$\tau(p \rightarrow \pi^0 e^+) \sim \frac{M_{\text{GUT}}^4}{m_p^5} \sim 10^{41} \text{ sec.} \quad (25)$$

If B' is similarly violated at the same high scale M_{GUT} , our DM techni-baryon would decay with life-time

$$\tau \sim \frac{M_{\text{GUT}}^4}{M_{\text{DM}}^5} \sim 10^{26} \text{ sec,} \quad (26)$$

which falls in the ball-park required by the phenomenological analysis above. Models of unification of the Standard Model couplings in the presence of a dynamical electroweak symmetry breaking mechanism have been recently explored [40, 41]. Interestingly, the scale of unification suggested by the phenomenological analysis emerges quite naturally [41].

Low energy DM and nucleon (quasi)-stability imply that, in the primeval Universe, at temperatures $T \lesssim M_{\text{GUT}}$ perturbative violation of the B' and B global charges is strongly suppressed. Since this temperature is presumably larger than the reheating temperature, it is unlikely that Ω_B and Ω_{DM} result directly from an asymmetry generated in B' or B . More likely, the initial seed yielding Ω_{DM} and Ω_B could be an initial asymmetry in lepton number L that, much along the lines of well studied leptogenesis scenarios [42], feeds the B and B'

asymmetries through the sphaleron effects.⁴ Indeed, it has been shown that it is possible to embed seesaw-types of scenarios in theories of dynamical symmetry breaking, while keeping the scale of the L -violating Majorana masses as low as $\sim 10^3$ TeV [46].

Assuming that techni-baryon DM decay is dominantly due to effective four-fermion operators, its decay modes significantly depend on the technicolor gauge group. In the following F generically denotes any SM fermion, quark or lepton, possibly allowed by the Lorentz and gauge symmetries of the theory.

- If the technicolor group is $SU(3)$, the situation is analogous to ordinary QCD: DM is a fermionic QQQ state, and effective $QQQF$ operators gives DM $\rightarrow \Pi^- \ell^+$ decays. This leads to hard leptons, but together with an excess of \bar{p} , from the $\Pi^- \rightarrow s\bar{c}$ decay (in view of $\Pi^- \simeq W_L^-$). This is therefore incompatible with PAMELA \bar{p} data, unless astrophysical propagation uncertainties are relaxed.
- If the technicolor group is $SU(4)$ the situation is typically worse: DM is a bosonic $QQQQ$ state, and effective $QQQQ$ operators lead to its decay into techni-pions.
- Finally, if the technicolor gauge group is $SU(2)$, DM is a bosonic QQ state, (as put forward in [24]), and effective $QQFF$ operators lead to DM decays into two F . Since the fundamental representation of $SU(2)$ is pseudoreal, one actually gets an interesting dynamics analyzed in detail in [24]. Here the technibaryon is a pseudo-Goldstone boson of the underlying gauge theory.

An $SU(2)$ technicolor model compatible with the desired features is obtained assuming that the left component of the Dirac field Q has zero hypercharge and is a doublet under $SU(2)_L$, so that DM is a scalar QQ with no weak interactions, and the four-fermion operator $(QQ)\partial_\mu(\bar{F}\gamma_\mu F)$ allows it to decay. Such operator is possible for both SM leptons and quarks, so that the DM branching ratios into $\ell^+\ell^-$ and $q\bar{q}$ is a free parameter.

The use of higher dimensional representations for the techniquarks transforming under a given technicolor gauge group has opened new possibilities [28]. Interestingly, the technicolor model with the lowest possible value for the naive S parameter (measuring deviations from electroweak precision data) can be constructed by combining *exactly* two Dirac flavors in the fundamental of $SU(2)$ with one Dirac in the adjoint representation (uncharged with respect to the SM) [24]. The model has also the lowest number of fermions and is compatible with near conformal dynamics, which is an important ingredient for reducing the tension with constraints stemming from unobserved flavor changing neutral currents.

6 Conclusions

We explored the interpretation of the excess of e^\pm cosmic rays observed by PAMELA and ATIC in terms of decays of Dark Matter with mass M_{DM} .

⁴In Minimal Walking Technicolor [43, 44], one additional (techni-singlet) $SU(2)$ -doublet must be introduced to cancel the odd-number-of-doublets anomaly [45]. An asymmetry in the L' global charge associated with these new states can also serve as a seed for the B and B' asymmetries.

On the phenomenological side, we found that any DM decay modes involving hard leptons can fit the PAMELA excess for $M_{\text{DM}} \gtrsim 200 \text{ GeV}$, while decay modes that give soft leptons with energy $E \ll M_{\text{DM}}$ together with \bar{p} need $M_{\text{DM}} \gtrsim 10 \text{ TeV}$. The peak present around 800 GeV in the $e^+ + e^-$ ATIC spectrum can be reproduced if $M_{\text{DM}} \sim 2 \text{ TeV}$ and for DM decays into $\mu^+ \mu^-, \tau^+ \tau^-$ (characteristic of boson DM) and into $W^\pm \ell^\mp$ where ℓ is any lepton (characteristic of fermion DM). However, the latter decays are disfavored by the PAMELA non-observation of an excess in the \bar{p} CR spectrum. Fermionic DM is allowed if it decays into $\ell^+ \ell^- \nu$.

DM annihilations compatible with the PAMELA excess tend to give a flux of γ rays above the HESS [17, 47, 48] bounds and a flux of synchrotron radiation above the Davies [18] bounds, unless the DM density profile $\rho(r)$ is significantly less steep as $r \rightarrow 0$ than the NFW profile. Whether or not this should be considered a problem depends on the the reliability of N -body simulations, and of their extrapolation to scales below 100 pc.

Anyhow, this issue is not present for DM decays, because they give DM signals proportional to ρ rather than to ρ^2 . The HESS observation of the Galactic Ridge region gives the dominant constraint, which is just below the needed sensitivity, and can be improved by performing an observation optimized for DM rather than for astrophysics.

On the theoretical side, we found that it is easy to invent decaying DM models compatible with the above features suggested by data, just because model-building is less severely constrained than in the case of DM annihilations.

More interestingly, if the DM density is due to an asymmetry analogous to baryon number broken at low energy by weak anomalies, then the value of the DM mass suggested by the $e^+ + e^-$ peak, $M_{\text{DM}} \sim 2 \text{ TeV}$, is also the one that naturally gives the observed ratio between the dark and baryonic matter densities $\Omega_{\text{DM}}/\Omega_B \sim 5$.

Indeed, in such a case electroweak sphalerons keep $n_{\text{DM}} \sim n_B$ down to $T \gtrsim M_{\text{DM}}$; below this temperature the DM density gets Boltzmann-suppressed, until sphalerons freeze-out at the temperature $T_* \sim 200 \text{ GeV}$. As a result, the correct DM density is obtained for $M \sim 8T_*$, which coincides with the mass suggested by the ATIC peak. Technicolor extensions of the SM suggest a similar value for the mass of the lightest (quasi)-stable state. Technicolor is a new strongly coupled gauge dynamics which breaks the electroweak symmetry dynamically and solves the hierarchy problem without an elementary Higgs. These models feature technibaryons which are quasi-stable technihadrons analogous to the proton in QCD, that possess, quite surprisingly, many of the required properties advocated by our phenomenological analysis.

While these phenomenological coincidences are indeed suggestive, from the theoretical point of view, bound states of some new strong dynamics decaying predominantly into leptons require some specific construction, that seems to privilege an $\text{SU}(2)$ technicolor gauge theory with a technimatter structure envisioned in [24].

References

- [1] PAMELA collaboration, [0810.4995](#).
- [2] ATIC collaboration, Nature 456 (2008) 362. See also PPB-BETS collaboration, [0809.0760](#). EC collaboration, proceedings of 1999 ICRC, Salt Lake City 1999, Cosmic ray, vol. 3, pag. 61–64.
- [3] PAMELA collaboration, [0810.4994](#).
- [4] HESS collaboration, [0811.3894](#).
- [5] M. Cirelli, M. Kadastik, M. Raidal, A. Strumia, [0809.2409](#).
- [6] M. Cirelli, R. Franceschini, A. Strumia, Nucl. Phys. B800 (2008) 204 [[0802.3378](#)].

- [7] L. Bergstrom, T. Bringmann and J. Edsjo, [0808.3725](#). V. Barger, W. Y. Keung, D. Marfatia and G. Shaughnessy, [0809.0162](#). I. Cholis, L. Goodenough, D. Hooper, M. Simet and N. Weiner, [0809.1683](#). M. Pospelov and A. Ritz, [0810.1502](#). A. E. Nelson and C. Spitzer, [0810.5167](#). Y. Nomura and J. Thaler, [0810.5397](#). R. Harnik and G. D. Kribs, [0810.5557](#). T. Hambye, [0811.0172](#). K. Ishiwata, S. Matsumoto, T. Moroi, [0811.0250](#). P. J. Fox and E. Poppitz, [0811.0399](#). E. Ponton and L. Randall, [0811.1029](#). S. Baek and P. Ko, [0811.1646](#).
- [8] N. Arkani-Hamed, D. P. Finkbeiner, T. Slatyer and N. Weiner, [0810.0713](#).
- [9] G. Bertone, M. Cirelli, A. Strumia, M. Taoso, [0811.3744](#). See also M. Regis and P. Ullio, Phys. Rev. D 78, 043505 (2008) [[0802.0234](#)]. N. F. Bell and T. D. Jacques, [0811.0821](#)
- [10] C.R. Chen, F. Takahashi, [0810.4110](#). P.-F. Yin, Q. Yuan, J. Liu, J. Zhang, X.-J. Bi, S.-H. Zhu, [0811.0176](#). A. Ibarra, D. Tran, [0811.1555](#). C.-R. Chen, F. Takahashi, T. T. Yanagida, [0811.3357](#).
- [11] T. Delahaye, R. Lineros, F. Donato, N. Fornengo and P. Salati, [0712.2312](#).
- [12] J. Hisano, S. Matsumoto, O. Saito, M. Senami, Phys. Rev. D 73 (2006) 055004 [[hep-ph/0511118](#)].
- [13] J. F. Navarro, C. S. Frenk and S. D. M. White, Astrophys. J. 462, 563 (1996) [[astro-ph/9508025](#)].
- [14] B. Moore, F. Governato, T. R. Quinn, J. Stadel and G. Lake, Astrophys. J. 499, L5 (1998) [[astro-ph/9709051](#)].
- [15] F. Donato, N. Fornengo, D. Maurin and P. Salati, Phys. Rev. D 69 (2004) 063501 [[astro-ph/0306207](#)].
- [16] HESS collaboration, [astro-ph/0307452](#).
- [17] HESS collaboration, [0711.2369](#).
- [18] R.D. Davis, D. Walsh, R.S. Booth, MNRAS 177 (1976) 319.
- [19] See A. Strumia, F. Vissani, [hep-ph/0606054](#) for a recent review.
- [20] WMAP collaboration, [0803.0547](#).
- [21] D. B. Kaplan, Phys. Rev. Lett. 68, 741 (1992).
- [22] S. M. Barr, R. S. Chivukula and E. Farhi, Phys. Lett. B 241, 387 (1990).
- [23] J. A. Harvey and M. S. Turner, Phys. Rev. D 42, 3344 (1990).
- [24] T. A. Ryttov and F. Sannino, arXiv:0809.0713 [[hep-ph](#)]. Published in Physics. Rev. D.
- [25] S. B. Gudnason, C. Kouvaris and F. Sannino, Phys. Rev. D 74, 095008 (2006) [[hep-ph/0608055](#)].
- [26] Y. Burnier, M. Laine and M. Shaposhnikov, JCAP 0602, 007 (2006) [[hep-ph/0511246](#)].
- [27] S. Nussinov, Phys. Lett. B 165, 55 (1985).
- [28] F. Sannino, [0804.0182](#)
- [29] J. M. Cline, M. Jarvinen and F. Sannino, Phys. Rev. D 78, 075027 (2008) [[0808.1512](#)].
- [30] M. E. Shaposhnikov, JETP Lett. 44, 465 (1986) M. E. Shaposhnikov, Nucl. Phys. B 287, 757 (1987).
- [31] K. Kajantie, M. Laine, K. Rummukainen and M. E. Shaposhnikov, Nucl. Phys. B 466, 189 (1996) [[hep-lat/9510020](#)].
- [32] J. M. Cline, [hep-ph/0609145](#).
- [33] S. Dimopoulos, D. Eichler, R. Esmailzadeh and G. D. Starkman, Phys. Rev. D 41, 2388 (1990). See also R. S. Chivukula and T. P. Walker, Nucl. Phys. B 329, 445 (1990).
- [34] D. O. Caldwell, R. M. Eisberg, D. M. Grumm, M. S. Witherell, B. Sadoulet, F. S. Goulding and A. R. Smith, Phys. Rev. Lett. 61, 510 (1988).
- [35] G. Rybka and P. Fisher, [hep-ex/0507086](#).
- [36] J. Bagnasco, M. Dine and S. D. Thomas, Phys. Lett. B 320 (99) 1994 [[hep-ph/9310290](#)].
- [37] CDMS collaboration, [0802.3530](#).
- [38] V.A. Rubakov, Nucl. Phys. B256 (1985) 509.
- [39] See e.g. J. Hisano, H. Murayama and T. Yanagida, Nucl. Phys. B 402, 46 (1993) [[hep-ph/9207279](#)].
- [40] N. D. Christensen and R. Shrock, Phys. Rev. D 72, 035013 (2005) [[hep-ph/0506155](#)].
- [41] S. B. Gudnason, T. A. Ryttov and F. Sannino, Phys. Rev. D 76, 015005 (2007) [[hep-ph/0612230](#)].
- [42] M. Fukugita and T. Yanagida, Phys. Lett. B 174, 45 (1986).
- [43] D. D. Dietrich, F. Sannino and K. Tuominen, Phys. Rev. D 72, 055001 (2005) [[hep-ph/0505059](#)].
- [44] R. Foadi, M. T. Frandsen, T. A. Ryttov and F. Sannino, Phys. Rev. D 76, 055005 (2007) [[0706.1696](#)].
- [45] E. Witten, Phys. Lett. B 117, 324 (1982).
- [46] T. Appelquist and R. Shrock, Phys. Lett. B 548, 204 (2002) [[hep-ph/0204141](#)].
- [47] HESS collaboration, [astro-ph/0601509](#).
- [48] HESS collaboration, [astro-ph/0603021](#).